Journal of Hazardous Materials 379 (2019) 120570

Contents lists available at ScienceDirect

Journal of Hazardous Materials

journal homepage: www.elsevier.com/locate/jhazmat

Effects of ferrihydrite nanoparticle incorporation in cementitious materials on radioactive waste immobilization

Shuai Fan[a,1], Bo Cao[b,1], Ning Deng[b,1], Yandi Hu[b,**,3], Mo Li[a,c,*,2]

[a] Department of Civil & Environmental Engineering, University of California, Irvine, CA, 92697, United States
[b] Department of Civil & Environmental Engineering, University of Houston, Houston, TX, 77004, United States
[c] Department of Chemical Engineering and Materials Science, University of California, Irvine, CA, 92697, United States

GRAPHICAL ABSTRACT

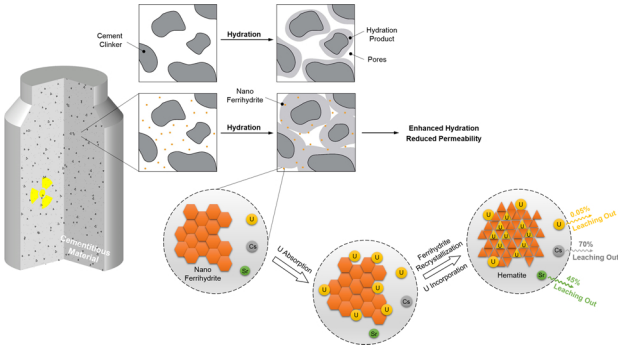

ARTICLE INFO

Keywords:
Ferrihydrite nanoparticles
Cement
Uranium
Strontium
Cesium

ABSTRACT

To enhance the long-term immobilization of radioactive wastes, ferrihydrite nanoparticles were incorporated into cementitious materials. The effects of ferrihydrite nanoparticles on the physicochemical and mechanical properties of cementitious materials and the immobilization of uranium (U), strontium (Sr) and cesium (Cs) were investigated. Adding ferrihydrite nanoparticles at 0.65%, 1.30%, 3.90% and 6.50% of cement weight slightly improved compressive strength by 5–11%, but dramatically reduced U leaching by 50–57%. The enhanced U immobilization was attributed to the strong adsorption of U by ferrihydrite nanoparticles, and the structural incorporation of U into hematite formed during ferrihydrite recrystallization. Although ferrihydrite nanoparticles had weaker effect than hematite nanoparticles on improving cement hydration and reducing permeability, they exhibit stronger U immobilization capacity. In contrast, incorporating ferrihydrite nanoparticles into cementitious materials had no significant effects on Cs and Sr leaching and no detectable adsorption of Sr and Cs. This study elucidated the fundamental differences in the interactions between ferrihydrite nanoparticles and U, Sr or Cs within cementitious systems that led to the distinctive immobilization mechanisms for these radionuclides. It generated new mechanistic understandings of U, Sr and Cs leaching from cementitious barriers modified by Fe-based nanoparticles, and proposed a new approach for enhancing long-term immobilization of U.

* Corresponding author at: Department of Civil and Environmental Engineering, E4145 Engineering Gateway, University of California, Irvine, CA 92697-2175, United States.
** Corresponding author at: Department of Civil & Environmental Engineering, University of Houston, TX, 77004, United States.
E-mail addresses: moli@uci.edu (M. Li), yhu11@uh.edu (Y. Hu).
[1] Equal contribution.
[2] http://engineering.uci.edu/users/mo-li.
[3] http://www.cive.uh.edu/faculty/hu.

https://doi.org/10.1016/j.jhazmat.2019.04.053
Received 14 December 2018; Received in revised form 30 March 2019; Accepted 14 April 2019
Available online 15 April 2019
0304-3894/

1. Introduction

Uranium (U), strontium (Sr) and cesium (Cs) are the most significant radionuclides in the waste inventory released into soils, sediments, and groundwater [1,2]. Subsurface environments contaminated with these radionuclides present severe health risks, and are extremely challenging for remediation. Cement-based immobilization systems have been adopted worldwide as a long-term storage and disposal approach for low- and intermediate-level radioactive wastes [3–17]. Cementitious material serves as a physical barrier and also a chemical binder for the radionuclides [3]. Interaction of cement with radionuclides during cement hydration within a high internal pH results in chemisorption of radionuclides onto cement, and co-precipitation and lattice incorporation in the major hydration products such as portlandite ($Ca(OH)_2$), calcium silicate hydrate (C-S-H in cement chemist notation), and ettringite [5,8], thus providing a binder effect. When incorporated in C-S-H, U is immobilized by sorption and co-precipitation [12]. In the presence of abundant silica, Sr is retained in C-S-H gel or ettringite by substituting the Ca^{2+} ions in the interlayer sites with the Sr^{2+} ions, where water enhances the possibilities for atomic bonding and charge transfer [5,13,14,18]. Cs can possibly be absorbed onto C-S-H but this binding effect is low at high pH or remain as free ions in the pore solution due to its high solubility [15–17].

Despite these immobilization mechanisms, the porous structure of cementitious materials can lead to gradual dissolution and leaching of radionuclides, posing challenges to long-term immobilization [10,11,19]. To enhance immobilization, pozzolanic ingredients have been introduced to cementitious materials, including fly ash, blast furnace slag, silica fume, ilmenite, calcined kaolin, and siliceous volcanic ash [20–27]. These ingredients either improve the physical properties of cementitious materials, such as reducing porosity and permeability, or increase the absorption of radionuclides with increased silica content. Besides pozzolanic siliceous and aluminous ingredients, our recent work [28] incorporated hematite (α-Fe_2O_3) nanoparticles into cementitious materials and found significantly reduced U leaching, attributed to both U adsorption on hematite nanoparticles and the refined pore structure of cementitious material. However, U adsorption to hematite can be reversed due to change in environmental conditions [29], causing radionuclide remobilization [6,10,29,30]. Therefore, in addition to physical adsorption, a mechanism based on structural incorporation of radionuclides is direly needed to enhance long-term immobilization.

Ferrihydrite is effective in sequestering contaminants due to its extremely high surface area and adsorption capability [31–34]. Also, under hydrothermal conditions, ferrihydrite was reported to recrystallize into thermodynamically more stable phases (goethite and hematite) [35], and structurally incorporate the adsorbed U during atom rearrangement [36–45]. This suggests that incorporating ferrihydrite nanoparticles into cementitious materials might enhance U immobilization through both physical adsorption and structural incorporation mechanisms. Meanwhile, ferrihydrite nanoparticles might affect cement hydration kinetics, thus altering cementitious material microstructure and properties, consequently promoting or inhibiting radionuclide leaching. Furthermore, although ferrihydrite has demonstrated high adsorption capacity for various metals [46–49], its interactions with Sr and Cs ions remain unknown.

This study filled the important knowledge gaps and tested the following hypotheses: (1) the interactions of U, Sr and Cs with ferrihydrite-cementitious systems are different, leading to their different leaching behaviors; (2) ferrihydrite and hematite nanoparticles differently affect cement hydration and the resulting material microstructure and properties, consequently influencing U, Sr and Cs leachability; (3) ferrihydrite-cementitious systems can better enhance U immobilization through both physical adsorption and structural incorporation of U. To test these hypotheses, leaching tests were performed on cementitious specimens containing ferrihydrite or hematite nanoparticles. To elucidate the physical and chemical mechanisms underlying the leaching phenomena, the effects of ferrihydrite nanoparticles on cement hydration, material permeability and compressive strength were studied; U, Sr, Cs adsorption on ferrihydrite nanoparticles and the ferrihydrite phase transformation under leaching conditions were investigated.

2. Materials and methods

2.1. Synthesis and characterization of ferrihydrite nanoparticles

Ferrihydrite nanoparticles were synthesized following the method in Leibl et al [50]. 100 *g* of $Fe(NO_3)_3{\cdot}9H_2O$ was dissolved in 1000 mL of 18.2 MΩ ultrapure water. Then, 1 M NaOH solution was added slowly with stirring to maintain pH of 10.0 ± 0.2 for 3 h to allow nanoparticle formation. Finally, the nanoparticles were collected through centrifugation, dialyzed against ultrapure water, dried under room temperature, and then ground and stored. X-ray diffraction (XRD, Miniflex600, Rigaku) was performed to characterize the crystallinity of the synthesized nanoparticles. The nanoparticle size was measured as 121 ± 16 nm by dynamic light scattering (Zetasizer Nano, Malvern). The chemical formula of the nanoparticles was estimated as $Fe_2O_3{\cdot}2.5\ H_2O$, by measuring the Fe content in dried ferrihydrite nanoparticles using atomic absorption spectroscopy (AAnalyst 200, PerkinElmer).

2.2. Preparation of ferrihydrite-cementitious specimens containing U, Sr, and Cs

Cementitious specimens containing U, Cs, and Sr and different amounts of ferrihydrite nanoparticles or hematite nanoparticles were prepared for leaching tests (Table 1). The specimens are labeled as C, C + 0.65%F, C + 1.30%F, C + 3.90%F, C + 6.50%F, and C + 1.00%H, where C indicates cement, F and H indicate ferrihydrite and hematite nanoparticles, respectively, and the number indicates the percentage weight ratio of nanoparticles to cement. Found in our previous study [28], adding 1.00 wt% hematite nanoparticles to cement showed the highest immobilization effect on U and thus is adopted as control in this study. Note that C + 1.00%H and C + 1.30%F had the same amount of Fe (0.36 wt%) for suitable comparison between cementitious specimens containing the two different types of Fe-based nanoparticles.

For each specimen, the radioactive waste solution (A) with U, Cs,

Table 1
Leaching test specimen compositions.

Specimen	Cement (g)	$UO_2(NO_3)_2{\cdot}\ 6H_2O$ (g)	$CsNO_3$ (g)	$Sr(NO_3)_2$ (g)	Ferrihydrite (g)	Hematite (g)	Fe (wt %)	Water (g)
C	50	1.85	0.72	0.78	–	–	0	25
C + 0.65%F	50	1.85	0.72	0.78	0.33	–	0.18	25
C + 1.30%F	50	1.85	0.72	0.78	0.65	–	0.36	25
C + 3.90%F	50	1.85	0.72	0.78	1.95	–	0.90	25
C + 6.50%F	50	1.85	0.72	0.78	3.25	–	1.80	25
C + 1.00%H	50	1.85	0.72	0.78	–	0.50	0.36	25

and Sr was prepared by dissolving 1.85 g $UO_2(NO3)_2{\cdot}6H_2O$, 0.72 g $CsNO_3$, 0.78 g $Sr(NO_3)_2$, and 4.20 g $NaNO_3$ in 20 mL ultrapure water. To prepare the suspension of well-dispersed ferrihydrite nanoparticles (B), 0.33, 0.65, 1.95 and 3.25 g dried ferrihydrite nanoparticles were added into 5 mL NaOH solution to adjust the pH = 10.0 and then sonicated for 10 min. Then, 20 mL solution (A) and 5 ml suspension (B) were added into 50 g Type I ordinary Portland cement (C) and mixed for 5 min to reach a well-dispersed, coherent state. The water-to-cement ratio was 0.5. The fresh mixture was cast into a cylinder mold (diameter = 2.2 cm, height = 1.8 cm), demolded after 24 h and then cured in a fume hood at 20 ± 1 °C and 45 ± 5% RH for 28 days before leaching tests.

2.3. Leaching tests of U, Cs and Sr

The leaching tests were conducted following the standard method of ANSI/ANS-16.1-R2017 [51]. The ferrihydrite-cementitious specimens containing U, Sr and Cs prepared in Section 2.2 were immersed in 200 mL ultrapure water at 90 °C, to mimic the high temperature caused by the decay of radionuclides. A ratio of leachate volume to cement surface area of 10.0 ± 0.2 was achieved as required by the standard [28,51]. The sampling time intervals were 2 h, 7 h, 1 d, 2 d, 3 d, 4 d, 5 d, 19 d, 47 d, 90 d and 170 d. After each sampling, the leachate was replaced with ultrapure water. The pH values of all leachates collected were measured to be 10.0 ± 0.3, which was due to the dissolution of $Ca(OH)_2$ from the cementitious material. The sampled leachates were then filtrated through 0.2 μm filters and acidified with 2% HNO_3. The dissolved U, Cs, and Sr concentrations were measured by inductively coupled plasma mass spectrometry (ICP-MS, PerkinElmer Elan Drc II).

2.4. Batch experiments of U, Sr, Cs adsorption on ferrihydrite nanoparticles

To investigate potential U, Sr and Cs adsorption on ferrihydrite nanoparticles during their leaching process, batch adsorption experiments of U, Sr and Cs on ferrihydrite nanoparticles were conducted at pH = 10.0 ± 0.1, the same pH as the leachate. If 1.85 g $UO_2(NO3)_2{\cdot}6H_2O$, 0.72 g $CsNO_3$ or 0.78 g $Sr(NO_3)_2$ were dissolved in 200 mL ultrapure water, the same amounts as the leaching tests, there would be no precipitation of Sr or Cs at pH = 10.0 based on Geochemist's Workbench calculation (GWB, Release 9.0, Aqueous Solutions LLC). However, U would form as sodium uranate ($Na_2U_2O_7$) precipitates and the dissolved concentration of UO_2^{2+} (uranyl) for ferrihydrite adsorption would be the equilibrated concentration as 1 mM UO_2^{2+}/L, corresponding to 0.1 g $UO_2(NO3)_2{\cdot}6H_2O$ dissolved in 200 ml solution [28]. Therefore, 0.1 g $UO_2(NO3)_2{\cdot}6H_2O$, or 0.72 g $CsNO_3$, or 0.78 g $Sr(NO_3)_2$ were dissolved in 200 mL solution and mixed with 0.33 g or 3.25 g ferrihydrite nanoparticles, corresponding to 0.65% and 6.5% ferrihydrite added to cement in Table 1. The solution was transferred to four 50 mL centrifugal test tubes and rotated for 48 h to reach the adsorption equilibrium. Then, the solution was passed through a 0.2 μm filter. The U, Cs and Sr concentrations in the filtered solution were analyzed using ICP-MS. The adsorption capacity of ferrihydrite nanoparticles was then calculated based on the mass balance of radionuclides before and after the adsorption experiments.

2.5. Batch experiments of U structural incorporation during ferrihydrite recrystallization

Structural incorporation of U into goethite (α-FeOOH) or hematite (Fe_2O_3) structures may occur through co-precipitation during ferrihydrite recrystallization under leaching condition.[45] The phase transformation of ferrihydrite nanoparticles in the cementitious specimen cannot be measured using XRD due to the trivial percentage of nanoparticles. Therefore, a batch experiment similar to Marshall et al. [45] was conducted to investigate potential ferrihydrite recrystallization to goethite or hematite under leaching condition and the incorporation of U in goethite or hematite structure during this process. A synthetic cement leachate solution was prepared with 0.06 g/L $Ca(OH)_2$ solution at pH = 10.0, the same as the leachate collected during the leaching experiments. The solution was sparged with N_2 to remove CO_2 [45]. Ferrihydrite nanoparticles were added into the cement leachate with a solid/solution ratio of 4 g/L. The suspension was then sonicated for 10 min and spiked with U with an initial concentration of 10 ppm. Based on Geochemist's Workbench (GWB, Release 9.0, Aqueous Solutions LLC) calculation, this initial concentration of U is below the solubility of any U(VI) related phase. Then, the suspension was placed in an oven at 90 °C for 15 days to mimic the leaching condition. After 15 days, the aged nanoparticles in the suspension were collected by centrifuging. The mineral phase of the aged nanoparticles was analyzed using XRD (Miniflex600, Rigaku) and compared with that of the fresh nanoparticles.

The fresh and aged nanoparticles were dissolved layer-by-layer by consecutive acid wash for 0.5 h, 1 h, 3 h, 6 h, 12 h and 24 h (dilute HNO_3 solution with pH = 3.0). After 24 h, the undissolved particles were collected and dissolved in 2% nitric acid for 168 h until all the particles dissolved and the concentrations of dissolved U and Fe in the acid solutions were measured by ICP-MS to calculate the atomic U/Fe ratio in each layer. The first acid wash produced the atomic U/Fe ratios in the surface layers ($R_{U/Fe,\ s}$); when the atomic ratio of U/Fe was stable during later consecutive acid wash, it represented the atomic U/Fe ratio in the inner lattice ($R_{U/Fe,\ l}$) of the nanoparticles [52,53].

2.6. Isothermal calorimetry of cement hydration kinetics

To understand the effect of ferrihydrite nanoparticles on cement hydration kinetics, isothermal calorimetry [54] (TAM AIR) was conducted to measure the thermal flux released during cement hydration. The sample compositions were the same as in Table 1, but without including U, Cs and Sr. The measurements were conducted at a constant temperature of 25 °C, with a sensitivity of ± 20 μW and an accuracy > 95%. Capsuled ampoules containing cement, together with syringe injectors containing preblended ferrihydrite nanoparticles with ultrapure water, were inserted into a sealed reaction channel. After a 12-hour equalization period, the nanoparticle solution was injected into the ampoule and mixed for 1 min. To exclude the exothermic effect caused by early rapid dissolution of cement clickers, the initial 15-minute calorimetry data were removed. The rate of heat and the cumulative heat released during hydration were measured and normalized by the solid weight to quantify the rate and degree of hydration.

2.7. Permeability tests on ferrihydrite-cementitious specimens

To determine the mechanisms responsible for U, Cs and Sr leaching from cementitious materials, questions arise as to whether ferrihydrite nanoparticles alter the pore structure and permeability of cementitious materials, in addition to radionuclides adsorption and structural incorporation. Therefore, permeability tests were conducted on ferrihydrite-cementitious specimens; water permeability reflects the porosity and pore connectivity within cementitious materials. The specimen compositions were shown in Table 1 but without including radionuclides. The fresh mixtures were cast into cylindrical molds (diameter = 76 mm, height = 152 mm), demolded after 24 h, and stored in an environmental chamber at 25 °C and 100% RH till 28-day age. Afterwards, each specimen was cut into 25 mm-thick slice specimens, which were then soaked in water for 7 days at 25 °C, to ensure a saturated condition and avoid shrinkage-induced microcracking. The

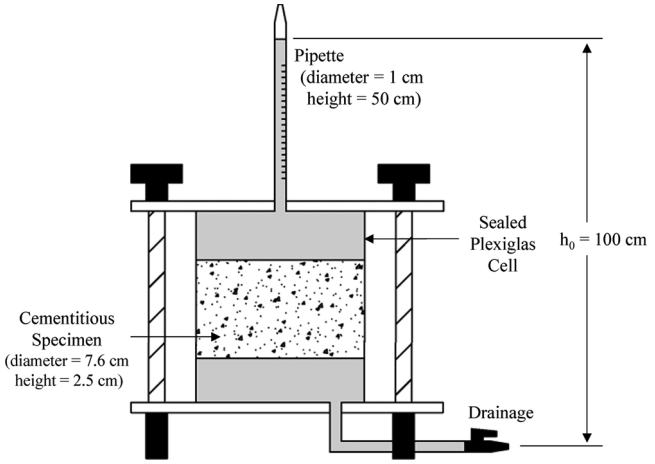

Fig. 1. Water permeability test.

specimens were then clamped in a permeability test apparatus (Fig. 1). During the test, the water height change with time was measured for up to 14 days. The permeability coefficient k was determined using Eq. (1), assuming laminar flow following Darcy's law [55].

$$k = (\frac{A^{'}d}{A\Delta t})ln(\frac{h_0}{h_t})k \quad (1)$$

where A is the specimen cross-sectional area, d is the specimen thickness, A' is the cross-sectional area of the pipette, Δt is the time required to reach a water head drop of $\Delta h = h_0 - h_t$, h_0 and h_t are water head height at the beginning and end of the test.

2.8. Compression tests on ferrihydrite-cementitious specimens

To understand the effect of ferrihydrite nanoparticles on the mechanical properties of cementitious materials, uniaxial compression tests were conducted [56]. The specimen compositions and preparation method were the same as the permeability tests. The suspension of well-dispersed ferrihydrite nanoparticles were added to Type I ordinary Portland cement together with additional water (water-to-cement ratio = 0.5), and mixed through a Hobart mixer for 5 min to reach a well-dispersed, coherent state. The fresh cement past was then cast into the cylinder mold (diameter = 76 mm, height = 152 mm). The specimens were demolded after 24 h and cured at a temperature of 20 ± 1 °C and relative humidity of 45 ± 5% till the age of 28 days for compressive testing. The compressive tests were conducted using a servohydraulic load frame (MTS) under displacement control at a rate of 0.025 mm/s, till the measured load dropped by 20% of the peak compressive load. The compressive strength was calculated by dividing the peak load by the initial cross-sectional area of the specimen. Three repeat specimens were tested for each mixture and the averages were reported.

3. Results

3.1. Leaching of U, Sr, and Cs from cementitious specimens

Fig. 2 shows the cumulative mass percentages of leached U, Sr, and Cs over a 170-day leaching period, and the diffusivity of U, Sr and Cs calculated based on the equation in ANSI/ANS-16.1–2003 (R2017). For the specimens without nanoparticles, the leaching of Cs was the fastest (70.8 ± 2.1%), followed by Sr (45.2 ± 0.9%), and then U whose 170-day leaching amount (0.104 ± 0.012%) was 2 orders of magnitude lower than Cs and Sr (Fig. 2**(a–c)**). This was consistent with the calculated effective diffusivities of U, Sr, and Cs (Fig. 2**(e)**). The diffusivity of Cs was the largest (~5×10^{-9} cm^2/s), followed by Sr (~1.8×10^{-9} cm^2/s) and U (~3×10^{-11} cm^2/s) that was 2 orders of magnitude lower than Cs and Sr.

In a cementitious matrix, the radionuclides can precipitate as insoluble salts, co-precipitate with cement hydration products, be adsorbed at hydrous surfaces, or exist as free ions in pore water [57]. The solubility of U in alkaline solution is very low, and more than 99% of U added in this experiment can precipitate as uranate complexes at pH = 10 based on GWB calculation. These complexes are physically encapsulated inside the cementitious matrix, thereby retarding U leaching [28]. Additionally, the remaining free UO_2^{2+} (uranyl) ions can be adsorbed onto the surfaces of cement mineral phases (e.g., SiO_2) and form an inner-sphere complex by sharing the equatorial oxygens, further reducing UO_2^{2+} leaching [58]. Different from U, the solubility of Sr is much higher under high pH, and thus cannot precipitate in the pore solution based on GWB calculation. Rather, Sr^{2+} can partially substitute Ca^{2+} in the ettringite structure [59,60]. Therefore, Sr leaching is retarded and partially controlled by the dissolution of ettringite. Cs has very high solubility in all pH conditions [59]. Cs tends to exist as free ions in the interstitial pore fluid of the cementitious matrix. Therefore, when the cementitious matrix is in contact with water, the leaching of free Cs ions becomes the fastest, compared with Sr and U whose leaching processes were retarded due to their different interactions with cement (for Sr and U), and the formation of insoluble precipitates (for U). These mechanisms are shown in Fig. 2**(d)**.

Compared with the control specimens without nanoparticles, the leached-out U from ferrihydrite-cementitious specimens decreased by ~50% after 170-day leaching (Fig. 2**(a)**). In contrast to U, the leaching rates of Sr and Cs were much higher and not significantly affected by the incorporation of ferrihydrite nanoparticles (Fig. 2**(b–c)**). The distinct leaching behaviors of U, Sr, and Cs suggested the fundamental differences in their interactions with ferrihydrite-cementitious materials, as further discussed in Section 4.1.

Finally, it was observed that different types of iron-based nanoparticles, hematite and ferrihydrite, differently affected U immobilization in cementitious materials. Compared with C + 1.00%H, the leached amounts of U from specimens containing 0.65–6.5% of ferrihydrite nanoparticles were all lower by ~30% (Fig. 2**(a)**). In contrast to U, no significant differences were observed for Sr and Cs leaching from cementitious materials containing hematite or ferrihydrite nanoparticles (Fig. 2**(b)** and **(c)**). These results suggested different interactions among the radionuclides (U, Sr, or Cs), the iron-based nanoparticles (ferrihydrite or hematite), and the cementitious materials. These mechanisms are further discussed in Section 4.3.

3.2. U, Sr, and Cs adsorption and structural incorporation by ferrihydrite

Table 2 shows 98 ± 1% of U but no detectable amount of Cs, Sr in solution was adsorbed on ferrihydrite nanoparticles. The adsorbed amounts of U were almost the same for 0.33 g and 3.25 g ferrihydrite nanoparticles, indicating that even the lowest amount of ferrihydrite nanoparticle incorporation (e.g., 0.65%) into cementitious materials was sufficient for adsorbing most of the dissolved U.

At high temperatures, ferrihydrite nanoparticles transform into more stable Fe (hydr)oxide mineral phases [61,62]. Marshall et al. [45] found that during ferrihydrite recrystallization into hematite under 60 °C, the adsorbed U on ferrihydrite was incorporated into the hematite structure [45]. In this study, the broad XRD spectra of the fresh nanoparticles (Fig. 3**(a)**) confirmed that these nanoparticles were 2-line ferrihydrite [63]. After aging in solution under the leaching temperature (90 °C) for 15 days (Fig. 3**(b)**), sharp diffraction peaks showed up at 2θ of 33°, 35°, 49°, and 54°, matching well with the characteristic diffraction peaks of hematite. This proved that ferrihydrite nanoparticles recrystallized to hematite under this study's leaching condition (90 °C).

To understand potential U incorporation into the aged hematite nanoparticles, consecutive acid wash experiments were conducted, and

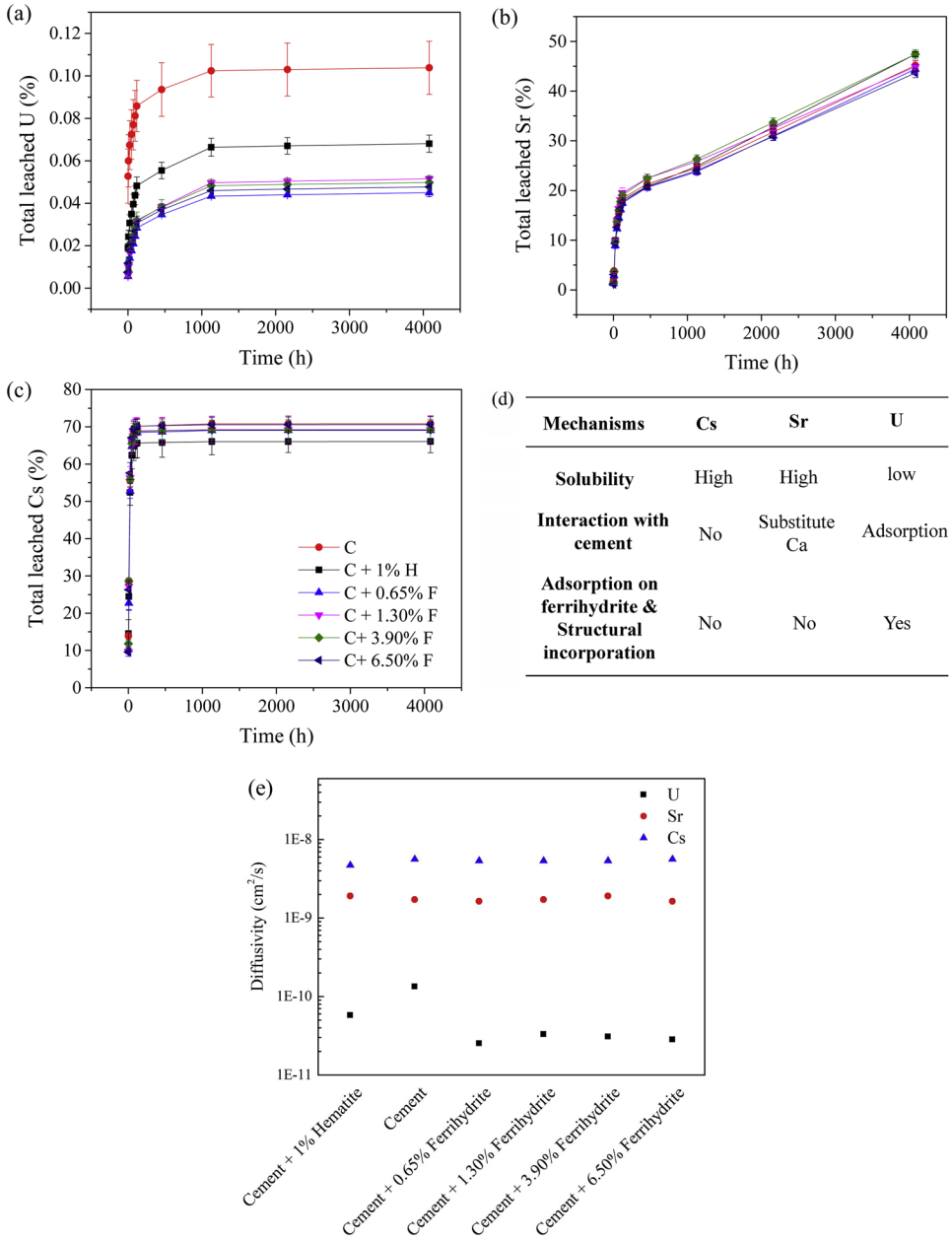

Mechanisms	Cs	Sr	U
Solubility	High	High	low
Interaction with cement	No	Substitute Ca	Adsorption
Adsorption on ferrihydrite & Structural incorporation	No	No	Yes

Fig. 2. The cumulative percentages of (a) U, (b) Sr, and (c) Cs leached from cementitious specimens, (d) the mechanisms controlling their leaching from cementitious material systems, and (e) effective diffusivities of U, Sr and Cs.

the atomic ratios of U/Fe on the surface ($R_{U/Fe,\ s}$) and in the lattice ($R_{U/Fe,\ l}$) of the fresh and aged nanoparticles are shown in Table 3. $R_{U/Fe,\ s}$ was high for both fresh (387 ± 20) and aged (207 ± 19) nanoparticles, indicating high adsorption capacities of U on both. $R_{U/Fe,\ l}$ for fresh ferrihydrite particles was 0 as U was below the detection limit. $R_{U/Fe,\ l}$ for the aged particles was 0.030 ± 0.003, indicating that significant amount of U was incorporated in the lattice structure of hematite during ferrihydrite recrystallization.

3.3. Effect of ferrihydrite and hematite nanoparticles on cement hydration

Fig. 4**(a)** shows the isothermal heat flow during cement hydration process. It was found that ferrihydrite nanoparticles accelerated cement reaction rate and also increased the peaks of hydration, which was primarily controlled by the rate at which the hydration products nucleated and grew. Nucleation effects have been found for other types of nano-size particles, such as nano-SiO_2, carbon nanotubes, nano-TiO_2,

Table 2
Absorbed U, Sr, and Cs on ferrihydrite nanoparticles.

Ferrihydrite (g)	U (%)	Cs (%)	Sr (%)
0.33 (as in C + 0.65%F)	98 ± 1	below detection limit	below detection limit
3.25 (as in C + 6.5%F)	98 ± 1	below detection limit	below detection limit

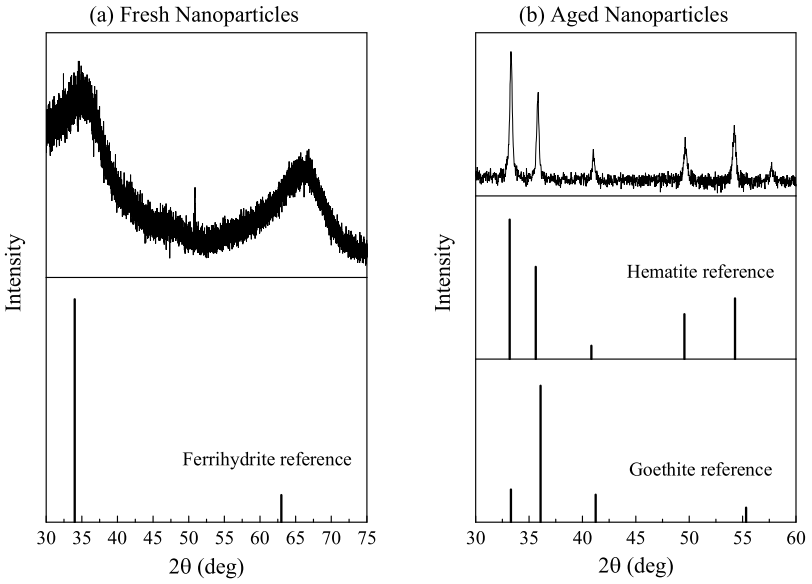

Fig. 3. XRD spectra of (a) fresh ferrihydrite and (b) aged nanoparticles.

Table 3
Chemical compositions of fresh and aged nanoparticles.

	U/Fe Molar Ratio	
Time (h)	Fresh Nanoparticles	Aged Nanoparticles
0.5 (Surface atomic U/Fe Ratio, $R_{U/Fe,\ s}$)	387 ± 20	207 ± 19
1	0.02 ± 0.01	89 ± 10
3	0.01 ± 0.01	58 ± 2
6	0	4.5 ± 0.5
12	0	0.025 ± 0.002
24	0	0.033 ± 0.003
Final (Lattice U/Fe Ratio, $R_{U/Fe,\ l}$)	0	0.030 ± 0.003

and nano-Fe_2O_3 [64]. This is the first time that nucleation effect was observed for ferrihydrite nanoparticles within cementitious materials. Fig. 4**(b)** shows the incorporation of ferrihydrite nanoparticles increased accumulative heat, indicating a higher degree of cement hydration during the first 120 h. The degree of hydration, α, was calculated by dividing the total amount of evolved heat at a given time (T) by the ultimate heat of reaction (Q_∞). Using a value of Q_∞ = 438 J/g that have been reported in literature [65], the estimated degrees of cement hydration at 1, 7, 14 and 28 days with different contents of iron-based nanoparticles are shown in Table 4.

Fig. 4 and Table 4 also shows that increasing ferrihydrite nanoparticles from 0.65% to 3.9% led to higher rate and degree of hydration, but this effect was reversed when the ferrihydrite content further increased from 3.9% to 6.5%. A possible explanation was that larger amount of nanoparticles led to particle agglomeration and consequently decreased their nucleation effect. By comparing the effects of two different iron (hydr)oxide nanoparticles, ferrihydrite and hematite, it was found that the hydration rate and degree were improved more notably by adding hematite over ferrihydrite nanoparticles. Compared with control pure cement, the peak heat flow increased by 19% for C + 3.90%F, but by 32% for C + 1.00%H.

3.4. Effects of ferrihydrite nanoparticles on cementitious material permeability and compressive strength

Fig. 5**(a)** shows the cumulated water flow permeation as a function of time for different cementitious specimens. After around 5 days, the steady water flow was reached. The water permeability coefficient, k,

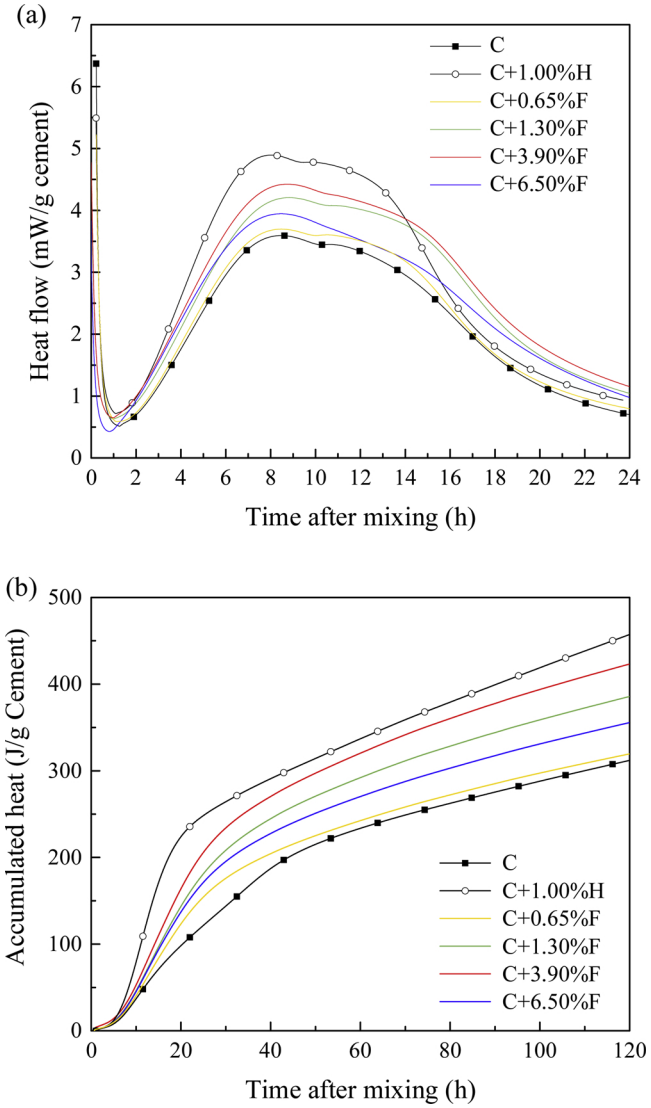

Fig. 4. Isothermal calorimetry on cement hydration. (a) Rate of heat evolution. (b) Accumulated heat with time.

Table 4
Degree of hydration (α) at different ages measured by isothermal calorimetry.

Specimen	α (1d)	α (7d)	α (14d)	α (28d)
C	0.30	0.62	0.69	0.72
C + 0.65%F	0.33	0.65	0.71	0.74
C + 1.30%F	0.35	0.68	0.75	0.78
C + 3.90%F	0.37	0.73	0.77	0.80
C + 6.50%F	0.34	0.66	0.73	0.75
C + 1.00%H	0.39	0.77	0.81	0.82

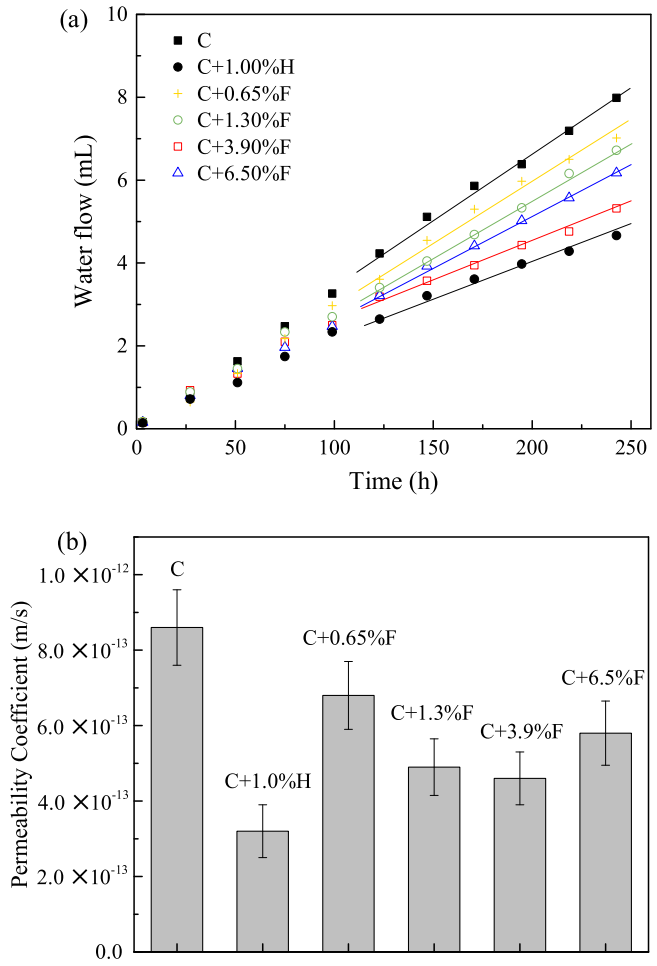

Fig. 5. Water permeability test results. (a) Water flow with time. (b) Permeability coefficients.

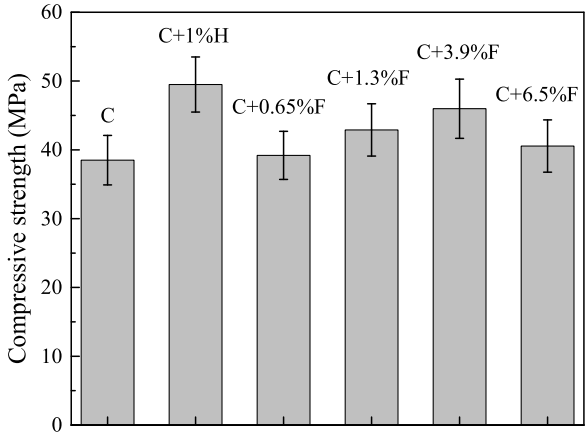

Fig. 6. 28-day compressive strength of cementitious materials.

was calculated using the slope of the linear line fitting the steady part of the permeation curve. Fig. 5**(b)** shows that adding ferrihydrite nanoparticles reduced the permeability of cementitious samples and this effect was the strongest in C + 3.90%F. It was also found that the specimen containing 1% hematite nanoparticles had the lowest permeability, compared with all specimens containing 0–6.5% ferrihydrite nanoparticles.

Fig. 6 shows that ferrihydrite nanoparticles improved the 28-day compressive strength of cementitious materials, with the largest improvement in C + 3.90%F. This effect by ferrihydrite nanoparticles, however, was not as significant as the cementitious materials containing 1% hematite nanoparticles.

These findings, together with isothermal calorimetry results, suggested that incorporation of ferrihydrite or hematite nanoparticles increased the degree of cement hydration, leading to denser microstructure and consequently lower permeability and higher compressive strength of cementitious materials; the optimum dosage of ferrihydrite nanoparticles was 3.90%. Moreover, the specimens containing 1% hematite nanoparticles had even stronger effect than those containing 0.65%–6.5% ferrihydrite nanoparticles.

4. Discussion

4.1. Incorporating ferrihydrite nanoparticles into cementitious materials retarded leaching of U, but not Sr or Cs

Dispersing small amounts (0.65–6.5%) of ferrihydrite nanoparticles into cementitious materials was found to reduce over 50% of U leaching (Fig. 2**(a)**). The enhanced U immobilization could be attributed to three major mechanisms: (1) adsorption on ferrihydrite nanoparticles, as evidenced in the batch experiments that 98% of U (Table 2) were adsorbed by even a small amount of ferrihydrite nanoparticles equivalent to 0.65 wt% of cement as in the leaching test specimens; (2) incorporation in hematite structure during ferrihydrite recrystallization into hematite under leaching conditions, validated by the change in $R_{U/Fe,\ l}$ from 0 in fresh ferrihydrite nanoparticles to 0.029 ± 0.004 in the aged nanoparticles (Table 3); and (3) lowered permeability of cementitious material, evidenced by accelerated cement hydration by ferrihydrite nanoparticles which led to denser microstructure of the hardened cementitious materials.

In contrast, incorporating ferrihydrite nanoparticles into cementitious materials did not significantly affect Sr or Cs leaching (Fig. 2). This was because Cs or Sr was either not absorbed onto ferrihydrite nanoparticles (Table 2) or structurally incorporated in hematite during ferrihydrite recrystallization. Therefore, the leaching of Cs or Sr was mainly governed by their interactions with the cementitious matrix. The faster leaching of Cs than Sr was due to the higher solubility of Cs that remains mostly as free ions in the cementitious pore solution.

4.2. The roles of Fe-based nanoparticles on cement hydration and material properties

Cement hydration process strongly influences the pore structure of cementitious materials, consequently affecting material transport properties (e.g. permeability) and mechanical properties (e.g. compressive strength). This study found that Fe-based nanoparticles, ferrihydrite and hematite, increased cement early-age hydration rate and degree. These nanoparticles acted as additional nucleation sites for the formation of cement hydration products, leading to lower permeability and higher compressive strength.

Hematite nanoparticles showed stronger effects than ferrihydrite nanoparticles on cement hydration and thus the permeability and mechanical strength. The possible mechanisms are: (1) the average size of hematite nanoparticles (~30 nm) was smaller than ferrihydrite nanoparticles (~120 nm), leading to more additional nucleation sites for cement hydration products; (2) the smaller particle size of hematite

resulted in a larger surface-to-volume ratio, thus lowering the surface energy barrier for the nucleation of cement hydration products on the nanoparticles; (3) ferrihydrite is an intermediate phase and thermodynamically less stable than hematite; therefore, it could participate in the cement hydration process to bond in hydrotalcite [66] and recrystallize to transform to hematite, thereby influencing the cement hydration kinetics.

XRD was performed to understand the effects of ferrihydrite nanoparticles on the compositions of cement hydration products. Fig. 7 Shows the X-ray diffraction spectra of 28-day cementitious samples containing 1% ferrihydrite nanoparticles, 1% hematite nanoparticles, or without any nanoparticles. The intensity was normalized into [0,1] range divided by the maximum peak counts. The XRD patterns did not show significant differences in the phase types. For example, the peaks at 2θ of 18°, 35°, 47°, and 51° corresponded to one of the major cement hydration products – calcium hydroxide (CH); the CH peaks were present in all mixtures. However, the relative peak intensities for CH and unhydrated cement clinkers (tricalcium silicate (C_3S) and dicalcium silicate (C_2S)), which have major peaks in the 2θ range of 29°-35°, varied among different samples. Table 5 shows the normalized intensity of CH at 2θ angle of 35° and unhydrated cement clinkers (C_3S/C_2S) at 33°. The peak intensity ratio between C_3S/C_2S and CH decreased from 0.85 for Cement-Control, to 0.68 and 0.78 for Cement + 1% Hematite and Cement + 1% Ferrihydrite, respectively. A lower peak intensity ratio between C_3S/C_2S and CH indicated that more cement clinkers (C_3S/C_2S) reacted during hydration. These XRD results supported the isothermal calorimetry results, suggesting that although ferrihydrite nanoparticles increased the degree of cement hydration, their effect was weaker than hematite nanoparticles.

Because this is the first study to understand the interaction among ferrihydrite nanoparticles, cement hydration and properties, and radionuclides leaching, the ferrihydrite-cementitious samples were designed without aggregates in order to reduce the complexity of the system and influencing parameters to reveal cement-ferrihydrite-radionuclides interactions. Also, this less complex system allowed us to relate the findings on cement hydration kinetics to the measured properties of cementitious materials and to the leaching phenomena. It is noted that concrete in structures typically have high content of aggregates. In addition to their effect on cement hydration, iron-based nanoparticles can also influence the aggregate-cement interfacial transition zone. Such effect will be investigated in future studies.

4.3. More effective U immobilization by incorporating ferrihydrite than hematite nanoparticles

This study revealed more effective U immobilization in cementitious materials by incorporating ferrihydrite nanoparticles than hematite nanoparticles (Fig. 2), despite that the latter had lower permeability. Three underlying mechanisms are discussed below.

First, the U adsorption capacities of ferrihydrite and hematite nanoparticles were compared. Ferrihydrite nanoparticles (121 ± 16 nm) had an adsorption capacity of 14.0 ± 0.1 mg U/g ferrihydrite. Hematite nanoparticles (30 nm) had an adsorption capacity of 16.3 ± 0.5 mg U/g hematite [67]. If expressed in mg U/g Fe, the adsorption capacities of ferrihydrite and hematite nanoparticles were 25.7 ± 0.2 and 23.3 ± 0.7 mg U/g Fe, respectively. The ferrihydrite nanoparticles in C + 1.30%F would adsorb only ~10% more U than the hematite nanoparticles in C + 1.00%H. However, the leached U from C + 1.30%F was ~30% lower than C + 1.00%H. Furthermore, based on batch adsorption experiments, U removal was all > 98% with varied amounts of ferrihydrite nanoparticles (Table 2), suggesting that the adsorption capacity difference between ferrihydrite and hematite nanoparticles should contribute to less than 10% of the U leaching difference from cementitious specimens. Therefore, the stronger U adsorption capacity of ferrihydrite than hematite nanoparticles was a contributing (< 10% difference) but not dominant mechanism for the greatly enhanced (~30%) U immobilization within cementitious materials.

Second, ferrihydrite and hematite nanoparticles affected cement hydration to different extent, thus differently influencing the pore structure of the hardened cementitious materials and the U leaching behavior. During cement hydration, U could be adsorbed onto the Fe-based nanoparticles, or incorporated in hydration products such as C-S-H by chemisorption and co-precipitation. The cementitious material pore structure, including the larger capillary pores and the finer gel pores that constitute the internal porosity of the C-S-H gel phase, affected the adsorption/desorption equilibrium between the free U ions in pore solution and the U adsorbed on Fe-based nanoparticles, as well as the dissolution/precipitation equilibrium between the free U ions in pore solution and the urinate precipitates. Therefore, the cementitious material pore structure affected the transport of U. This study found that the permeability of C + 1.30%F was higher than that of C + 1.00%H (Fig. 6). However, the leached U from C + 1.30%F was 30% lower than that from C + 1.00%H. This indicated that although hematite nanoparticles had stronger effects than ferrihydrate nanoparticles on accelerating cement early hydration and reducing the material porosity and permeability, these effects were not the dominant mechanisms for the enhanced U immobilization in ferrihydrite-cementitious materials.

Finally and most importantly, ferrihydrite nanoparticles were more effective than hematite nanoparticles in immobilizing U due to U incorporation in the lattice structure of hematite phase during ferrihydrite recrystallization. Adsorption process can be reversible and the adsorbed U can be desorbed and leached out from the cementitious system with time, but the structurally incorporated U is more irreversible due to the high stability of hematite structure under high pH conditions. Structural incorporation of U is the dominant mechanism for the enhanced and more permanent immobilization of U in ferrihydrite-cementitious materials.

5. Conclusions

The leaching behaviors of U, Cs, and Sr from cementitious materials incorporating ferrihydrite nanoparticles were investigated and compared with those incorporating hematite nanoparticles or without any nanoparticles. Various techniques were employed to characterize cement hydration, permeability, mechanical strength and radionuclide leaching. Fundamental understandings were gained on the radionuclides-nanoparticle-cement interactions, and their relations with radionuclides leaching behaviors.

Incorporating ferrihydrite nanoparticles into cementitious materials significantly enhanced U immobilization, due to both U adsorption on

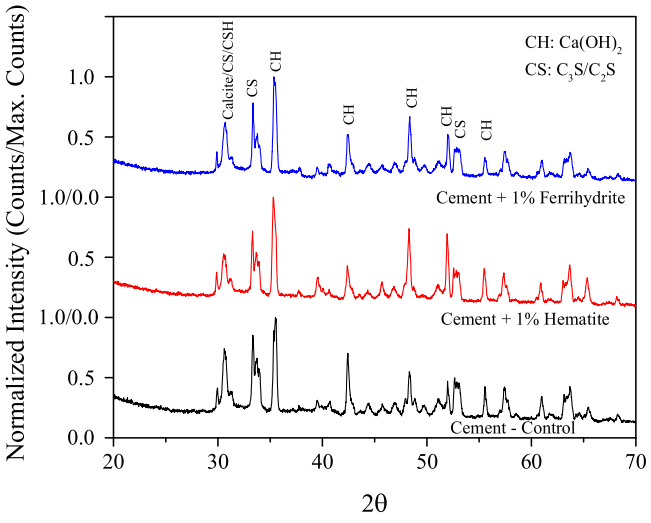

Fig. 7. XRD patterns of cementitious samples.

Table 5
Normalized peak intensity of unhydrated cement clinker C_3S/C_2S and hydration product $Ca(OH)_2$.

Samples	Normalized Intensity	
	C_3S/C_2S at 33°	$Ca(OH)_2$ at 35°
Cement-Control	0.85	1.0
Cement + 1% Hematite	0.68	1.0
Cement + 1% Ferrihydrite	0.78	1.0

ferrihydrite nanoparticles and the lattice incorporation of U into hematite structure during ferrihydrite recrystallization under leaching conditions. In contrast, the incorporation of ferrihydrite nanoparticles did not significantly affect Sr or Cs immobilization, because there was no significant adsorption or structural incorporation of Sr or Cs by ferrihydrite nanoparticles. These different interactions between ferrihydrite nanoparticles and U, Sr or Cs led to the distinctive immobilization mechanisms for these radionuclides in ferrihydrite-cementitious materials.

The incorporation of ferrihydrite nanoparticles affected cement hydration kinetics, leading to higher early-age hydration rate and degree. This consequently influenced the pore structure, transport and mechanical properties of the cementitious material. Although these positive effects were less significant in ferrihydrite-cementitious materials than hematite-cementitious materials, the former achieved significantly enhanced U immobilization due to the structural incorporation of U–a mechanism more stable and permanent than physical adsorption of U. This study provided new fundamental understandings about the interactions of different iron-based nanoparticles with different radionuclides within cementitious materials. These understandings shed light on designing better strategies for enhanced, long-term immobilization of radioactive wastes in cementitious systems.

Acknowledgements

We acknowledge funding from the U.S. Department of Energy, Office of Nuclear Energy, Nuclear Energy University Program (DE-AC07-05ID14517, #168284), and U.S. Department of Energy, Office of Science, Biological and Environmental Research (DE-AC02-05CH11231). We thank Dr. Mark A. Torres at Rice University for helping with ICP-MS measurements.

References

[1] R.G. Riley, J.M. Zachara, Chemical Contaminants on DOE Lands and Selection of Contaminant Mixtures for Subsurface Science Research (No. DOE/ER–0547T), Pacific Northwest Lab., Richland, WA (United States), 1992.
[2] D.O. Energy, Assessment of Disposal Options for DOE-Managed High-Level Radioactive Waste and Spent Nuclear Fuel, Department of Energy, Washington, DC, 2014.
[3] S. Komarneni, D.M. Roy, Mechanisms of immobilization of nuclear waste elements by cement minerals, cement and mortar, Cem. Concr. Res. 11 (5-6) (1981) 789–794.
[4] F.P. Glasser, Progress in the immobilization of radioactive wastes in cement, Cem. Concr. Res. 22 (2-3) (1992) 201–216.
[5] M. Atkins, F.P. Glasser, Application of Portland cement-based materials to radioactive waste immobilization, Waste Manag. 12 (2-3) (1992) 105–131.
[6] D.E. Macphee, F.P. Glasser, Immobilization science of cement systems, MRS Bull. 18 (03) (1993) 66–71.
[7] A. Kindness, A. Macias, F.P. Glasser, Immobilization of chromium in cement matrices, Waste Manag. 14 (1) (1994) 3–11.
[8] M.L.D. Gougar, B.E. Scheetz, D.M. Roy, Ettringite and C-S-H Portland cement phases for waste ion immobilization: a review, Waste Manag. 16 (4) (1996) 295–303.
[9] A.M. El-Kamash, A.M. El-Dakroury, H.F. Aly, Leaching kinetics of 137 Cs and 60 Co radionuclides fixed in cement and cement-based materials, Cem. Concr. Res. 32 (11) (2002) 1797–1803.
[10] B. Batchelor, Overview of waste stabilization with cement, Waste Manag. 26 (7) (2006) 689–698.
[11] S. Paria, P.K. Yuet, Solidification–stabilization of organic and inorganic contaminants using Portland cement: a literature review, Environ. Rev. 14 (4) (2006) 217–255.
[12] L.P. Moroni, F.P. Glasser, Reactions between cement components and U (VI) oxide, Waste Manag. 15 (3) (1995) 243–254.
[13] W. Gashier, T. Miura, K. Hashimoto, R.J. Hand, H. Kinoshita, Leaching behaviour of cementitious nuclear wasteforms containing caesium and strontium, Adv. Appl. Ceram. 113 (8) (2014) 447–452.
[14] R.D. Spence, Chemistry and Microstructure of Solidified Waste Forms, CRC Press, 1992.
[15] S. Bagosi, L.J. Csetenyi, Caesium immobilization in hydrated calcium-silicate-aluminate systems, Cem. Concr. Res. 28 (12) (1998) 1753–1759.
[16] S. Holgersson, Y. Albinsson, B. Allard, H. Borén, I. Pavasars, I. Engkvist, Effects of gluco-isosaccharinate on Cs, Ni, Pm and Th sorption onto, and diffusion into cement, Radiochim. Acta 82 (s1) (1998) 393–398.
[17] G. Bar-Nes, A. Katz, Y. Peled, Y. Zeiri, The mechanism of cesium immobilization in densified silica-fume blended cement pastes, Cem. Concr. Res. 38 (5) (2008) 667–674.
[18] M. Gavrilescu, L.V. Pavel, I. Cretescu, Characterization and remediation of soils contaminated with uranium, J. Hazard. Mater. 163 (2) (2009) 475–510.
[19] R. Pabalan, F. Glasser, D. Pickett, G. Walter, S. Biswas, M. Juckett, L. Sabido, J. Myers, Contract NRC NRC-02-07-006, CNWRA, 2009, p. 1.
[20] A. Guerrero, S. Goni, Efficiency of a blast furnace slag cement for immobilizing simulated borate radioactive liquid waste, Waste Manag. 22 (7) (2002) 831–836.
[21] A. Fernández-Jiménez, D.E. Macphee, E.E. Lachowski, A. Palomo, Immobilization of cesium in alkaline activated fly ash matrix, J. Nucl. Mater. 346 (2) (2005) 185–193.
[22] T.S. Singh, K.K. Pant, Solidification/stabilization of arsenic containing solid wastes using Portland cement, fly ash and polymeric materials, J. Hazard. Mater. 131 (1) (2006) 29–36.
[23] A.E. Osmanlioglu, Immobilization of radioactive waste by cementation with purified kaolin clay, Waste Manag. 22 (5) (2002) 481–483.
[24] K. Sakr, M.S. Sayed, N. Hafez, Comparison studies between cement and cement-kaolinite properties for incorporation of low-level radioactive wastes, Cem. Concr. Res. 27 (12) (1997) 1919–1926.
[25] A. Dyer, T. Las, M. Zubair, The use of natural zeolites for radioactive waste treatment: studies on leaching from zeolite/cement composites, J. Radioanal. Nucl. Chem. 243 (3) (2000) 839–841.
[26] A.M. El-Kamash, M.R. El-Naggar, M.I. El-Dessouky, Immobilization of cesium and strontium radionuclides in zeolite-cement blends, J. Hazard. Mater. 136 (2) (2006) 310–316.
[27] Q. Sun, J. Li, J. Wang, Effect of borate concentration on solidification of radioactive wastes by different cements, Nucl. Eng. Des. 241 (10) (2011) 4341–4345.
[28] B. Cao, S. Fan, X. Tan, M. Li, Y. Hu, Cementitious materials modified with hematite nanoparticles for enhanced cement hydration and uranium immobilization, Environ. Sci. Nano 4 (8) (2017) 1670–1681.
[29] U.R. Berner, Evolution of pore water chemistry during degradation of cement in a radioactive waste repository environment, Waste Manag. 12 (2-3) (1992) 201–219.
[30] P. Zhou, B. Gu, Extraction of oxidized and reduced forms of uranium from contaminated soils: Effects of carbonate concentration and pH, Environ. Sci. Technol. 39 (12) (2005) 4435–4440.
[31] G.A. Waychunas, B.A. Rea, C.C. Fuller, J.A. Davis, Surface chemistry of ferrihydrite: Part 1. EXAFS studies of the geometry of coprecipitated and adsorbed arsenate, Geochim. Cosmochim. Acta 57 (10) (1993) 2251–2269.
[32] T.D. Waite, J.A. Davis, T.E. Payne, G.A. Waychunas, N. Xu, Uranium (VI) adsorption to ferrihydrite: Application of a surface complexation model, Geochim. Cosmochim. Acta 58 (24) (1994) 5465–5478.
[33] K.P. Raven, A. Jain, R.H. Loeppert, Arsenite and arsenate adsorption on ferrihydrite: kinetics, equilibrium, and adsorption envelopes, Environ. Sci. Technol. 32 (3) (1998) 344–349.
[34] F.M. Michel, L. Ehm, S.M. Antao, P.L. Lee, P.J. Chupas, G. Liu, D.R. Strongin, M.A. Schoonen, B.L. Phillips, J.B. Parise, The structure of ferrihydrite, a nanocrystalline material, Science 316 (5832) (2007) 1726–1729.
[35] S. Das, M.J. Hendry, J. Essilfie-Dughan, Transformation of two-line ferrihydrite to goethite and hematite as a function of pH and temperature, Environ. Sci. Technol. 45 (1) (2010) 268–275.
[36] T. Sato, T. Murakami, N. Yanase, H. Isobe, T.E. Payne, P.L. Airey, Iron nodules scavenging uranium from groundwater, Environ. Sci. Technol. 31 (10) (1997) 2854–2858.
[37] J.E. Stubbs, D.C. Elbert, D.R. Veblen, C. Zhu, Electron microbeam investigation of uranium-contaminated soils from Oak Ridge, TN, USA, Environ. Sci. Technol. 40 (7) (2006) 2108–2113.
[38] D.E. Giammar, J.G. Hering, Time scales for sorption− desorption and surface precipitation of uranyl on goethite, Environ. Sci. Technol. 35 (16) (2001) 3332–3337.
[39] S.C. Smith, M. Douglas, D.A. Moore, R.K. Kukkadapu, B.W. Arey, Uranium extraction from laboratory-synthesized, uranium-doped hydrous ferric oxides, Environ. Sci. Technol. 43 (7) (2009) 2341–2347.
[40] M.C. Duff, J.U. Coughlin, D.B. Hunter, Uranium co-precipitation with iron oxide minerals, Geochim. Cosmochim. Acta 66 (20) (2002) 3533–3547.
[41] P.S. Nico, B.D. Stewart, S. Fendorf, Incorporation of oxidized uranium into Fe (hydr)oxides during Fe (II) catalyzed remineralization, Environ. Sci. Technol. 43 (19) (2009) 7391–7396.
[42] B.D. Stewart, P.S. Nico, S. Fendorf, Stability of uranium incorporated into Fe (hydr) oxides under fluctuating redox conditions, Environ. Sci. Technol. 43 (13) (2009) 4922–4927.
[43] D.D. Boland, R.N. Collins, T.E. Payne, T.D. Waite, Effect of amorphous Fe (III) oxide transformation on the Fe (II)-mediated reduction of U (VI), Environ. Sci. Technol. 45 (4) (2011) 1327–1333.

[44] E.S. Ilton, J.S.L. Pacheco, J.R. Bargar, Z. Shi, J. Liu, L. Kovarik, M.H. Engelhard, A.R. Felmy, Reduction of U (VI) incorporated in the structure of hematite, Environ. Sci. Technol. 46 (17) (2012) 9428–9436.
[45] T.A. Marshall, K. Morris, G.T. Law, F.R. Livens, J.F.W. Mosselmans, P. Bots, S. Shaw, Incorporation of uranium into hematite during crystallization from ferrihydrite, Environ. Sci. Technol. 48 (7) (2014) 3724–3731.
[46] Y. Song, P.J. Swedlund, N. Singhal, Copper (II) and cadmium (II) sorption onto ferrihydrite in the presence of phthalic acid: some properties of the ternary complex, Environ. Sci. Technol. 42 (11) (2008) 4008–4013.
[47] P. Trivedi, J.A. Dyer, D.L. Sparks, Lead sorption onto ferrihydrite. 1. A macroscopic and spectroscopic assessment, Environ. Sci. Technol. 37 (5) (2003) 908–914.
[48] M.F. Schultz, M.M. Benjamin, J.F. Ferguson, Adsorption and desorption of metals on ferrihydrite: reversibility of the reaction and sorption properties of the regenerated solid, Environ. Sci. Technol. 21 (9) (1987) 863–869.
[49] P. Trivedi, J.A. Dyer, D.L. Sparks, K. Pandya, Mechanistic and thermodynamic interpretations of zinc sorption onto ferrihydrite, J. Colloid Interface Sci. 270 (1) (2004) 77–85.
[50] H. Leibl, R. Tomasits, P. Brühl, A. Kerschbaum, M.M. Eibl, J.W. Mannhalter, Humoral and cellular immunity induced by antigens adjuvanted with colloidal iron hydroxide, Vaccine 17 (9-10) (1999) 1017–1023.
[51] ANSI/ANS-16.1-2003, American Nuclear Society Committee, 2003.
[52] C. Dai, X. Zuo, B. Cao, Y. Hu, Homogeneous and heterogeneous $(Fe_x, Cr_{1-x})(OH)_3$ precipitation: implications for Cr sequestration, Environ. Sci. Technol. 50 (4) (2016) 1741–1749.
[53] C. Dai, Y. Hu, Fe (III) hydroxide nucleation and growth on quartz in the presence of Cu (II), Pb (II), and Cr (III): metal hydrolysis and adsorption, Environ. Sci. Technol. 49 (1) (2014) 292–300.
[54] ASTM C1679, Standard Practice for Measuring Hydration Kinetics of Hydraulic Cementitious Mixtures Using Isothermal Calorimetry, ASTM International, 2009.
[55] D.C. Hughes, Pore structure and permeability of hardened cement paste, Mag. Concr. Res. 37 (133) (1985) 227–233.
[56] ASTM C617/C617M – 15, Standard Practice for Capping Cylindrical Concrete Specimens, ASTM International, 2015.
[57] N.D.M. Evans, Binding mechanisms of radionuclides to cement, Cem. Concr. Res. 38 (4) (2008) 543–553.
[58] E.R. Sylwester, P.G. Allen, P. Zhao, B.E. Viani, Interactions of uranium and neptunium with cementitious materials studied by XAFS, MRS Online Proceedings Library Archive, (1999), p. 608.
[59] R.A. Rahman, D.Z. El Abidin, H. Abou-Shady, Cesium binding and leaching from single and binary contaminant cement–bentonite matrices, Chem. Eng. J. 245 (2014) 276–287.
[60] M. Youssef, R.J.M. Pellenq, B. Yildiz, Docking 90Sr radionuclide in cement: an atomistic modeling study, Phys. Chem. Earth Parts A/B/C 70 (2014) 39–44.
[61] Y. Cudennec, A. Lecerf, The transformation of ferrihydrite into goethite or hematite, revisited, J. Solid State Chem. 179 (3) (2006) 716–722.
[62] U. Schwertmann, J. Friedl, H. Stanjek, From Fe (III) ions to ferrihydrite and then to hematite, J. Colloid Interface Sci. 209 (1) (1999) 215–223.
[63] V.A. Drits, B.A. Sakharov, A.L. Salyn, A. Manceau, Structural model for ferrihydrite, Clay Miner. 28 (1993) 185-185.
[64] F. Sanchez, K. Sobolev, Nanotechnology in concrete–a review, Constr. Build. Mater. 24 (11) (2010) 2060–2071.
[65] I. Pane, W. Hansen, Investigation of blended cement hydration by isothermal calorimetry and thermal analysis, Cem. Concr. Res. 35 (2005) 1155–1164.
[66] B.Z. Dilnesa, E. Wieland, B. Lothenbach, R. Dähn, K.L. Scrivener, Fe-containing phases in hydrated cements, Cem. Concr. Res. 58 (2014) 45–55.
[67] H. Zeng, A. Singh, S. Basak, K.U. Ulrich, M. Sahu, P. Biswas, J.G. Catalano, D.E. Giammar, Nanoscale size effects on uranium (VI) adsorption to hematite, Environ. Sci. Technol. 43 (5) (2009) 1373–1378.